Eur Biophys J (2008) 37:333–344
DOI 10.1007/s00249-007-0251-2

ORIGINAL PAPER

Metal effects on the membrane interactions of amyloid-β peptides

John D. Gehman · Caitlin C. O'Brien · Fazel Shabanpoor · John D. Wade · Frances Separovic

Received: 20 September 2007 / Revised: 8 November 2007 / Accepted: 20 November 2007 / Published online: 25 January 2008

Abstract Aβ(1–42) peptide, found as aggregated species in Alzheimer's disease brain, is linked to the onset of dementia. We detail results of ^{31}P and ^{2}H solid-state NMR studies of model membranes with Aβ peptides and the effect of metal ions (Cu^{2+} and Zn^{2+}), which are found concentrated in amyloid plaques. The effects on the lipid bilayer and the peptide structure are different for membrane incorporated or associated peptides. Copper ions alone destabilise the lipid bilayer and induce formation of smaller vesicles, but not when Aβ(1–42) is associated with the bilayer membrane. Aβ(25–35), a fragment from the C-terminal end of Aβ(1–42), which lacks the metal coordinating sites found in the full length peptide, is neurotoxic to cortical cortex cell cultures. Addition of metal ions has little effect on membrane bilayers with Aβ(25–35) peptides. ^{31}P magic angle spinning NMR data show that Aβ(1–42) and Aβ(1–42)-Cu^{2+} complexes interact at the surface of anionic phospholipid membranes. Incorporated peptides, however, appear to disrupt the membrane more severely than associated peptides. Solid-state ^{13}C NMR was used to compare structural changes of Aβ(1–42) to those of Aβ(25–35) in model membrane systems of anionic phospholipids and cholesterol. The Aβ peptides appeared to have an increase in β-strand structure at the C-terminus when added to phospholipid liposomes. The inclusion of Cu^{2+} also influenced the observed chemical shift of residues from the C-terminal half, providing structural clues for the lipid-associated Aβ/metal complex. The results point to the complex pathway(s) for toxicity of the full-length peptide.

Keywords Amyloid Aβ · Cholesterol · Metal interactions · Peptide–lipid interactions · Phospholipid membranes · Solid-state NMR · Structure · Alzheimer's disease

Abbreviations

AD	Alzheimer's disease
APP	Amyloid precursor protein
(CP)MAS	(Cross-polarisation) Magic angle spinning
CQ	Clioquinol
CSA	Chemical shift anisotropy
HFIP	Hexafluoroisopropanol
LUV	Large unilamellar vesicles
MLV	Multilamellar vesicles
NMR	Nuclear magnetic resonance
(*d*)POPC	*sn-1* (deuterated) Palmitoyl, *sn-2* oleoyl phosphatidylcholine
POPS	Palmitoyloleoylphosphatidylserine
REDOR	Rotational-echo double resonance
SS-NMR	Solid-state NMR

Introduction

Alzheimer's disease (AD) is a neurodegenerative disorder (Alzheimer 1907) associated with the accumulation of the

Australian Society for Biophysics Special Issue: Metals and Membranes in Neuroscience.

J. D. Gehman · C. C. O'Brien · F. Shabanpoor · F. Separovic (✉)
School of Chemistry, Bio21 Institute,
The University of Melbourne, Melbourne, VIC 3010, Australia
e-mail: fs@unimelb.edu.au

F. Shabanpoor · J. D. Wade
Howard Florey Institute, University of Melbourne,
Melbourne, VIC 3010, Australia

β-amyloid peptide (Aβ) as aggregated, insoluble plaques in the brain. These plaques are the most distinctive pathology of AD, which has led to intensive study of Aβ peptides. These peptides (Fig. 1) result from the cleavage of the transmembrane Amyloid Precursor Protein (APP) by γ- and β-secretases, and vary in size from 39 to 43 amino acid residues (Kang et al. 1987; Glenner and Wong 1984; Masters et al. 1985; Sisodia 1992). While both Aβ(1–40) and Aβ(1–42) are the predominant forms found in cerebral tissue of afflicted patients, their aggregation and cytotoxicity properties are significantly different (Harper and Lansbury 1997). As Aβ(1–40) is also found in non-AD afflicted brain, its presence may be unconnected to the disease pathogenesis (Roher et al. 1993). Thus far, our studies have focused on the longer and more toxic Aβ(1–42) (Burdick et al. 1992; Zhang et al. 2002). We have also studied Aβ(25–35) due to the observation of similar toxic effects to 'full length' peptide (Varadarajan et al. 2001; Barnham et al. 2003) while aggregating at different rates. Aβ(25–35) also allows studies to focus on that portion of the Aβ peptide which is transmembrane in the context of the intact APP (Kang et al. 1987; Coles et al. 1998).

Although much has been made of the insoluble properties of the peptide, current opinion is that soluble forms of Aβ are more likely to be responsible for toxicity (Donnelly et al. 2007; Kayed et al. 2003; Lesné et al. 2006; McLean 1999). Soluble oligomeric species of Aβ(1–42) have been shown to promote lipid release from cells (Demeester et al. 2000), and there is only weak correlation between the amount of Aβ plaques and the extent of neurodegeneration (Christian et al. 2007; Hartley et al. 1999; Lambert. 1998; Tickler et al. 2005), further strengthening the supposition that soluble forms of Aβ are the neurotoxic species that lead, at least initially, to the observed neurodegeneration.

Several potential mechanisms resulting in disruption by Aβ of nerve cell function have been identified. These include both direct disruption of membrane structure and facilitating oxidative damage to membrane and other cellular components. This activity, which employs mainly copper (Cu^{2+}) as a redox cofactor, could oxidize macromolecules either indirectly by formation of reactive oxygen species, or directly by involving components in the catalytic redox cycle (Barnham et al. 2004; Smith et al. 2006, 2007). Specific Aβ/Cu^{2+} interactions appear to be important for this destructive mechanism, through the coordination of three His sidechain nitrogens and one of a number of different possible oxygens as discussed below. Membrane interactions are also strongly correlated with the deleterious effects of Aβ on nerve cell function, even where oxidative damage may occur only indirectly. Further, membrane interactions are implicated in the formation of insoluble amyloid fibrils, suggesting that amyloid may be a by-product of the initially damaging interactions between lipid and peptide (Choo-Smith et al. 1997).

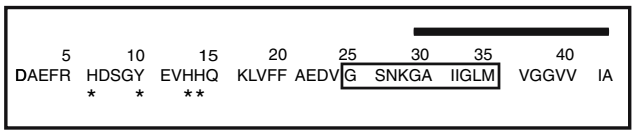

Fig. 1 Human Aβ(1–42) sequence. *Boxed region* indicates Aβ(25–35) fragment. *Asterisk* denotes probable metal-coordinating residues. *Solid bar* denotes portion of Aβ(1–42) which is transmembrane in the context of APP

As metals are implicated in AD, they are often targets for treatment of the disease. Copper, zinc and iron are found in high concentrations in amyloid plaques (Bush 2003). EPR data has indicated that these metals are able to coordinate to Aβ peptides through the histidine residues at positions 6, 13 and 14, and the tyrosine residue at position 10 (Smith et al. 2006). Cu^{2+} has been found to increase Aβ toxicity, and when the imidazole side chain nitrogens of histidine were methylated, Aβ toxicity was attenuated owing to the disabling of metal coordination (Smith et al. 2006). The effect of copper has been investigated and the Cu^{2+}/peptide ratio for aggregate formation and toxicity is proposed to be 1:1 (Ali et al. 2004; Smith et al. 2006).

Methionine at Aβ(1–42) position 35 has also been identified as a significant determinant in Aβ pathology (Barnham et al. 2003). While it has been implicated in the oxidation/reduction activity of the peptide, and mutation to structurally similar norleucine results in reduced oxidative damage in cell, however, extending the C-terminal Met35 of Aβ(25–35) by Val36, which lacks metal-coordination sites, also reduces oxidative damage (Varadarajan et al. 2001).

Our research concentrates on solid-state NMR (SS-NMR) studies of the amyloid peptide Aβ(1–42) and the fragment Aβ(25–35) in phospholipid bilayers and the effect of metal ions (Cu^{2+} and Zn^{2+}). Although a solid-state NMR structure of Aβ(1–40) in the fibril form has been determined by Tycko and co-workers (Petkova et al. 2002), the structural form of this pleomorphic peptide (Lau et al. 2003) in a membrane bilayer has yet to be determined. In addition to the peptide–lipid interaction, we report structural studies in model membrane systems and the effect of the metal ions on the peptide structure. Structural changes of Aβ incorporated within and associated with a model membrane are compared.

Experimental

Materials

Synthetic deuterated *sn*-1 palmitoyl, *sn*-2 oleoyl phosphatidylcholine (*d*POPC), palmitoyloleoylphosphatidylcholine

(POPC) and palmitoyloleoylphosphatidylserine (POPS), were purchased from Avanti Polar Lipids (Alabaster, USA) and used without further purification. Cholesterol was purchased from Sigma Aldrich (St Louis, USA). $^{13}C_1$-Gly, $^{13}C_1$-Ala, and $^{13}C_2$-Leu were purchased from Cambridge Isotope Laboratories (Andover, USA). FMOC-succinamide was purchased from Auspep (Melbourne, Australia) and FMOC-protected amino acids were synthesized and purified as previously described (Lau et al. 2007b). Labelled, protected amino acids were incorporated into positions Gly29, Ala30, Leu34 of Aβ(1–42) and analogous positions of Aβ(25–35) by solid phase peptide synthesis as described previously (Lau et al. 2007b). Aβ(1–42) had the sequence DAEFR HDSGY EVHHQ KLVFF AEDVG SNK[$^{13}C_1$-G] [$^{13}C_1$-A] IIG[1^3C_2-L]M VGGVV IA, and Aβ(25–35) had the sequence SNK[$^{13}C_1$-G] [$^{13}C_1$-A] IIG[$^{13}C_2$-L]M. Peptides were purified by reverse phase HPLC and were identified by mass spectrometry with *m/z* of 4518.4 for Aβ(1–42) and *m/z* of 1064.3 for Aβ(25–35).

Sample preparation

Generally, multilamellar vesicles (MLV) were prepared either by dissolving equal stoichiometric amounts of (*d*)POPC and POPS, or (*d*)POPC, POPS and cholesterol, in chloroform and methanol (9:1), drying into a thin film under reduced pressure, and further drying under high vacuum overnight. MLV were formed upon rehydration with up to 0.5 mL (0.05 M) Tris–HCl buffer (pH = 7) followed by freeze–thawing the suspension typically 4–5 times between liquid N_2 and a 40°C water bath. The samples were then bench centrifuged at 12,000*g* for 20 min. and the supernatant removed.

Aβ(1–42) and Aβ(25–35) were dissolved in hexafluoroisopropanol (HFIP) at a ratio of 1 mL HFIP to 1 mg of peptide. Peptide was dried into a thin film as for lipids above. Where peptide was *incorporated* in the formation of MLV bilayers, lipid in organic solvent was added to this thin film of peptide at the beginning of the MLV preparation (above). Where peptide was *associated* with vesicles after MLV preparation, the preformed vesicles were slurried on top of the dry peptide film. A total lipid/peptide mole ratio of 30:1 was used. ^{19}F NMR was used to confirm that TFA did not remain from peptide synthesis, and only insignificant amounts of HFIP (<0.5% mol/mol-peptide) remained from the initial dissolution of peptide.

Where Cu^{2+} was added, an appropriate volume of 0.1 M copper glycine ($CuGly_2$) solution, prepared by dissolving 1:2 mole ratio of $CuCl_2$ with glycine in water, was added to the peptide/MLV sample between the second and third of four freeze thaw cycles. A 1:1 (mol/mol) metal to peptide ratio was used.

SS-NMR

NMR experiments were conducted on a Varian (Palo Alto, USA) Inova 300 or VNMRS 600 spectrometer using 5 mm HX AutoMAS and 3.2 mm BioMAS probes, respectively. All experiments were conducted at a controlled air temperature of 28°C. ^{13}C cross-polarisation magic angle spinning (CPMAS) (Stejskal et al. 1977) experiments at 4–7 kHz MAS were conducted using recycle delays of 2 or 4 s (for 75.5 and 150.8 MHz, respectively), cross polarisation contact times of 1 or 2 ms (for 75.5 and 150.8 MHz, respectively), ^{13}C constant CP spin lock field of 45–50 kHz, ^{1}H spin lock at the −1 sideband match condition, optimised on adamantane, and 56 kHz CW or 67 kHz SPINAL64 (Fung et al. 2000) ^{1}H decoupling (for 75.5 and 150.8 MHz, respectively). The "static" ^{31}P experiment was conducted on the VNMRS 600 spectrometer in the same rotor and probe as for the ^{13}C experiments. ^{31}P spectra was collected using a Hahn-echo pulse sequence with 6 s recycle delay, 4.4 μs $\pi/2$ pulse width, and 60 μs effectual total echo time; spectral width was set to ~420 kHz, and the acquisition started early in the second half of the echo such that the FID could be manually left-shifted to the top of the echo and subsequently downsampled by a factor of 5. SPINAL64 decoupling as for ^{13}C CPMAS experiments was applied during the echo and acquisition.

NMR of membranes: background

Model membrane systems

Naturally occurring membrane systems are complicated mixtures of phospholipids, sterols, proteins, glycolipids, gangliosides and sphingomyelin (Singer and Nicolson 1972). While more naturally occurring mixtures of lipids can be employed (e.g. Separovic et al. 2004), more often simplified membrane systems are used. These model membranes capture the significant characteristics of natural membranes such as acyl chain dynamics, diverse surface charge, sterol content and hydration levels, while allowing more definitive characterization of membrane structure and dynamics.

Model membranes used for these studies were primarily composed of phospholipids, which are a major component of cell membranes. Phospholipids are characterized by a hydrophilic phosphate headgroup attached to hydrophobic acyl chains. Our studies employed palmitoyl (16:0), and oleoyl (18:1) acyl chains at the *sn*-1 and *sn*-2 positions, respectively, with the unsaturated site ensuring that the membranes remain in the liquid lamellar phase through a range of different conditions. Although typically used in

equal proportions, the zwitterionic phosphatidylcholine headgroup (POPC) creates bulk lipid, while the negatively charged phosphatidylserine (POPS) provides at least negative charge density on the membrane surface, and possibly also a specific Aβ membrane binding potential associated with apoptosis (Demeester et al. 2000).

Cholesterol is also frequently included in our model membrane systems, as it is also found in biological membranes and has been specifically implicated in the pathology of AD (Sparks et al. 1990). Conflicting results have been reported regarding the role of cholesterol in AD. On one hand, Aβ toxicity has been reported to be both attenuated in cholesterol-enriched cells, and enhanced in cholesterol-depleted cells (Arispe and Doh 2002). On the other hand, in vivo (Fassbender et al. 2001), in vitro (Subasinghe et al. 2003) and epidemiological (Jick et al. 2000) studies suggest that lower levels correlate with a slowing of AD pathogenesis; hence Aβ interactions in phospholipid bilayers containing cholesterol were also studied.

While membrane bilayer structures vary from oriented planar bilayers and small to giant unilamellar vesicles, multilamellar (MLV) and large unilamellar vesicles (LUV) are most appropriate to study Aβ interactions with phospholipid bilayers. The typical diameter of an MLV is of the order of 5 μm (Watwe and Bellare 1995). Due to their size, MLV can be more closely related to a biological membrane and curvature effects are reduced and allow use of solid state-NMR techniques. LUV have diameters typically of 0.5 μm and were used in selected experiments.

Solid-state nuclear magnetic resonance spectroscopy

Solid state NMR is uniquely suited to the study of membrane systems and peptide–lipid interactions. It is a powerful complement to established approaches in structural biology, as it does not require long range crystalline order to gain structure information, as required for diffraction studies, and is not restricted by hydrodynamic properties as is NMR of molecules in solution. The relaxed constraints on sample preparation enable the study of structural and dynamic aspects of membrane-interacting peptides (Balla et al. 2004; Cornell et al. 1983) with respect to both peptide and the membrane bilayer than commonly used detergents provide in conventional structural approaches.

Phosphorous and deuterium SS-NMR are used to study the effect of the peptides on phospholipid headgroups and chains (Cornell et al. 1988; Balla et al. 2004), respectively, using acyl-deuterated phosphatidylcholine (PC). Specifically ^{13}C labelled residues were used to study changes in structure of the Aβ peptide with anionic phospholipid bilayers.

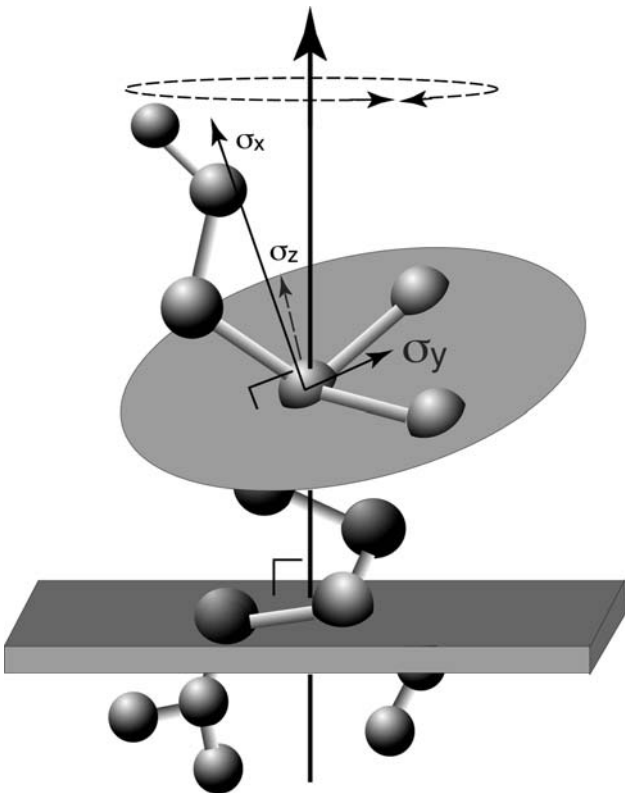

Fig. 2 Approximate orientation of ^{31}P chemical shift tensor with respect to the phosphodiester molecular segment of phospholipid headgroups

Static ^{31}P SS-NMR

The spin 1/2 ^{31}P isotope of phospholipid headgroups is ~100% naturally abundant, and consequently provides an easy probe of lipid phase and headgroup perturbation. In the absence of motion, static solid state ^{31}P NMR spectra of minimally hydrated phospholipid is governed by the chemical shift tensor, σ, most simply described in the diagonal basis with characteristic orthogonal axes oriented with reference to the phosphorus and two non-esterified oxygens and self-referenced to zero average frequency. This frame (Fig. 2) gives $\sigma_x \approx -81$ ppm, approximately perpendicular to the plane formed by the phosphorus and oxygens; $\sigma_y \approx -23$ ppm, approximately bisecting the bond angle formed by phosphorus and oxygens; and $\sigma_z \approx 104$ ppm, approximately the vector connecting the non-esterified oxygens to form a right-handed axis system (Griffin et al. 1978; Herzfeld et al. 1978; Kohler and Klein 1976). The static ^{31}P lineshape is defined by two edges corresponding to the extreme tensor component values and maximum intensity at the intermediate value.

In the presence of motion, such as the fast axial rotation of lipids about their long axis within liquid lamellar bilayers, the full chemical shift anisotropy observed in static ^{31}P NMR spectra becomes partially averaged to an axially

symmetric lineshape (Fig. 3) defined by edges "perpendicular" and "parallel" to the axis of rotation (Mehring 1983). The chemical shift anisotropy (CSA) is the difference between these two edges, and is an indicator of head group orientation and dynamics for membrane components under varying conditions. Headgroup orientation can be characterized by angles ϑ_x and ϑ_z from the lipid axis of rotation of σ_x and σ_z, respectively. These angles transformed (Gehman and Separovic 2006) into Euler angles,

$$\alpha = \cos^{-1}\left(\frac{\cos\vartheta_x}{\sin\vartheta_z}\right) = \sin^{-1}\left[\left(\sin^2\vartheta_x - \frac{\cos^2\vartheta_z\cos\vartheta_x}{\sin^2\vartheta_z}\right)^{1/2}\right] \quad (1)$$

and $\beta = \vartheta_z$, can be used to rotate the ^{31}P principal axis system into the frame where $\sigma_z = \sigma_{\|}$ is parallel to the lipid rotation axis, and the rotational motion averages the other tensor components to block diagonal degenerate values $\sigma_\perp$ oriented orthogonal to the lipid fast rotation axis. Ultimately,

$$\Delta\sigma = \left(\sigma_{\|} - \sigma_\perp\right) = \frac{3\cdot\chi}{2}\left[\sigma_x^{\mathrm{PAS}}\left(1-\cos^2\alpha\sin^2\beta\right) + \sigma_y^{\mathrm{PAS}}\left(1-\sin^2\alpha\sin^2\beta\right) + \sigma_z^{\mathrm{PAS}}\sin^2\beta\right], \quad (2)$$

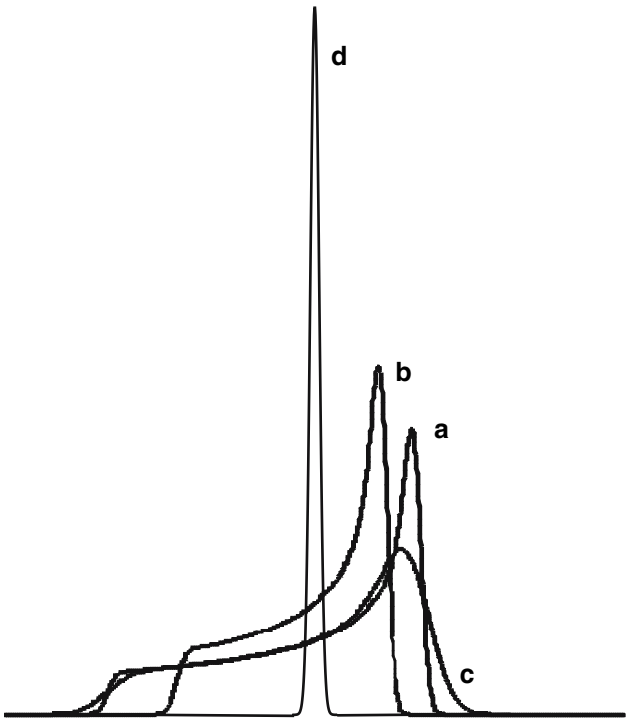

Fig. 3 Typical ^{31}P "powder patterns" for vesicle bilayers in the liquid-lamellar phase. The static lineshape may be relatively broad as in **a**, or narrower as in **b**, broadened due to increased T_2 relaxation mechanisms to that in **c**, or due to motional averaging be reduced to an isotropic component as in **d**, or any combination of the above

where a factor of χ is included to account for several additional modes of disorder of phospholipids in the liquid lamellar state (Dufourc et al. 1992; Kohler and Klein 1977; Griffin et al. 1978). Values of $\chi = 0.66$ are typical (Seelig and Gally 1976). Figure 4 shows the correlation between angular combinations within the subspace considered most physically likely based upon dipalmitoylphosphatidylcholine (Griffin et al. 1978) and for the range in CSA values centred on those discussed herein. For example CSA values of $\Delta\delta \sim -43$ may correlate to a range of angular combinations from approximately $\vartheta_x = 55°$ and $\vartheta_z = 90°$, to $\vartheta_x = 30°$ and $\vartheta_z = 90 \pm 25°$. Increases in CSA magnitude (e.g. Fig. 3a relative to b) may correspond to the headgroup tending toward being more upright (decreasing ϑ_x), and/or the non-esterified oxygen vector rotating closer to the plane of the bilayer (ϑ_z moving closer to 90°). Alternatively, or additionally, increased or decreased disorder represented by χ may also account for variations in observed CSA.

Other differences that may be observed in ^{31}P SS-NMR static spectra from unoriented bilayers suggest membrane interactions, which can effect low frequency motions (Cornell et al. 1983), giving a relaxation-broadened pattern, (Fig. 3c relative to a). As well, isotropic 'spikes' may form, which infers much more rapid reorientation or tumbling than for MLV, and averages out orientation dependent dipole and chemical shift interactions. These types of motions are typically observed in micelles, sonicated vesicles and cubic phases.

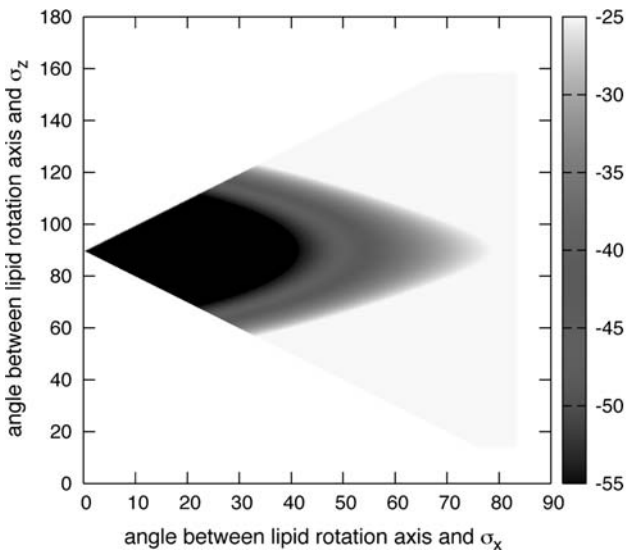

Fig. 4 Correlation of calculated ^{31}P CSA to headgroup orientation under lipid long-axis rotation

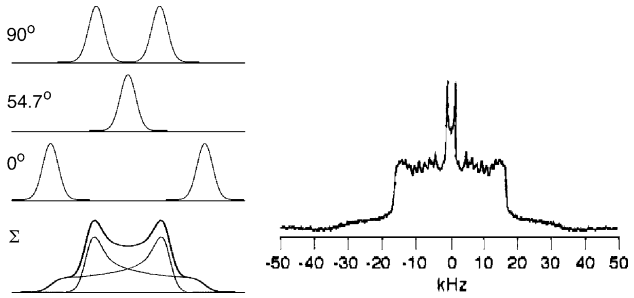

Fig. 5 (*Left*) Simulations of ^{2}H spectra obtained from different orientations of C–^{2}H bonds (90°, 54.7° and 0°), and the bottom spectrum being the result of a 'powder' with all orientations relative to the magnetic field. (*Right*) Spectrum is a typical ^{2}H SS-NMR spectrum of a perdeuterated phospholipid

Static ^{2}H SS-NMR

In contrast to the ~100% natural abundance of ^{31}P, the spin 1 ^{2}H isotope is virtually absent at natural abundance and permits the observation of introduced ^{2}H labels with little or no background. The C–^{2}H bond of a deuterated lipid acyl position oriented at a single angle θ relative to the applied magnetic field yields a doublet separated by a $(3\cos^2\theta-1)$-modulated quadrupolar splitting (Fig. 5). Each deuterated acyl position of a vesicle bilayer-distribution of lipids contributes a 'Pake' pattern (Pake 1948) in which mirror symmetric components are separated by the angular dependent quadrupolar splitting. This angular dependence also serves to attenuate the overall quadrupolar splitting to an extent characteristic of C–^{2}H bond disorder. Order varies between acyl positions, generally decreasing from the top of the chain to the terminal CD_3 position, and static ^{2}H SS-NMR spectra of lipids with several deuterated chain positions are a sum of Pake patterns from each (Fig. 5). ^{2}H SS-NMR experiments can consequently be used to detect perturbations to the dynamics of bilayer acyl chains according to membrane composition (e.g. the inclusion of cholesterol or variously unsaturated chains) or the addition of peptides.

Relaxation measurements

T_1 and T_2 measurements in general are used to help understand the motions of molecules. T_1, or longitudinal relaxation is a function of the intensity of motion at the Larmor or resonant frequency and, therefore, serves as an indicator of fast frequency motions, e.g. 121 MHz at 7.05 T for ^{31}P relaxation measurements. T_2, or transverse relaxation is complementary information, as it is an indicator of motion at 'zero' frequency, whereby slower motions serve to increase relaxation rates. For ^{31}P relaxation measurements of phospholipids within a bilayer, changes in fast motions report on dynamics experienced by individual lipids, and changes in slow frequency motions report on the collective motions of the bilayer surface (Dufourc et al. 1992; Separovic et al. 2000).

Magic angle spinning NMR

In NMR of molecules tumbling rapidly in solution, the anisotropy of chemical shift and dipolar coupling are averaged such that relatively narrow peaks are observed at the isotropic chemical shift. Magic angle spinning of solid or semi-solid (e.g. hydrated MLV) samples about an angle 54.74° to the applied magnetic field mechanically accomplishes a similar effect (Andrew et al. 1958, 1959; Lowe 1959). For spin ½ nuclei other than proton, CSA is typically the dominating spectral feature; typical MAS rates remove all apparent dipolar coupling, while the CSA is modulated into a manifold of spinning sidebands (Herzfeld and Berger 1980; Maricq and Waugh 1979) separated by the spin rate, particularly at higher applied magnetic field strengths. This allows spectral resolution of nuclei for which static lineshapes would have otherwise hopelessly overlapped. Furthermore, the isotropic chemical shift, or centre-band position (the peak within the manifold which does not move with changing MAS rate) is itself a strong indicator of torsion angles, which define local structure with respect to rotations about covalent bonds, most prominently for backbone nuclei of protein and peptide (Saitô 1983; Saitô et al. 1998).

Developing SS-NMR techniques

As the SS-NMR field develops, stronger magnetic fields have increased detection sensitivity, and advances in pulsed field spectrometer technology is expanding the range of potential techniques available. For example, rotational-echo double resonance (REDOR) and Boltzmann's Statistics REDOR are proving to be useful in calculating internuclear distances (Gehman et al. 2007). As SS-NMR allows membrane systems to be in a quasi-natural state, conformational changes can be examined by comparing changes in internuclear distances.

Results and discussion

Addition of Aβ to membrane systems

Aβ is added to vesicle bilayers by either 'incorporation' or 'association'. In the incorporated method, Aβ was added to the phospholipids prior to the formation of the vesicles by

dissolving peptide and lipids together in organic solvent, dried together into a thin film, and hydrated to form MLV. Alternatively, as in previous work (Lau et al. 2007a, b), peptide can be added in HFIP to preformed vesicles to 10% final concentration of HFIP, lyophilized, and rehydrated to destabilize then reform vesicle structure in the presence of peptide. In the associated method, Aβ is added to the phospholipid bilayers after the vesicles have been formed. Due to the tendency of Aβ to aggregate in solution, when associated, Aβ possibly also aggregates but in a manner templated by the phospholipid vesicle surface. Preparing the samples using the incorporated method favours peptide/lipid interactions, which may preclude, slow or chaperone the peptide/peptide interactions characteristic of larger aggregates. If the peptide does eventually aggregate regardless of the method of addition, the incorporated method gives the Aβ peptide a greater chance to aggregate according to a pathway that perhaps better imitates the natural process, beginning with its generation by secretase cleavage within the membrane. This offers greater prospects for observing how membrane interactions are involved in the Aβ pathogenesis. Experimentally, similar but more severe perturbations were often observed when the peptide was incorporated rather than associated into the membrane system.

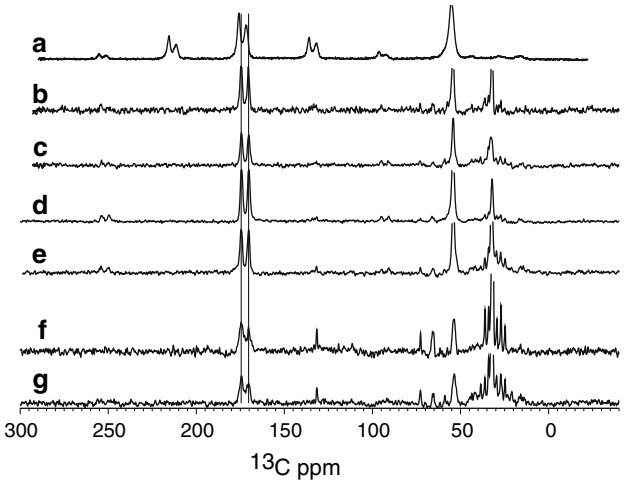

Fig. 6 ^{13}C CPMAS NMR spectra of: **a** dry Aβ(25–35); **b** associated Aβ(25–35) with POPC/POPS; **c** associated Aβ(25–35) with POPC/POPS/cholesterol; **d** incorporated Aβ(25–35) with POPC/POPS; **e** incorporated Aβ(25–35) with POPC/POPS/cholesterol; **f** incorporated Aβ(1–42) with POPC/POPS; **g** incorporated Aβ(1–42) with POPC/POPS/cholesterol. A peptide/POPC/POPS mole ratio of 1:15:15 was used and for peptide/POPC/POPS/cholesterol 1:10:10:10. All spectra were collected at a controlled air temperature of 28°C and 6 kHz MAS at 7.05 T for (**b**–**g**) and 14.1 T for (**a**). Dry peptide was not HFIP treated, which resulted in chemical shifts intermediate between HFIP-induced helical shifts (Lau et al. 2007a) and lipid-induced extended conformation shifts

Membrane interactions of Aβ(1–42) and the amyloidogenic fragment Aβ(25–35)

The impact of Aβ(1–42) when associated with *d*POPC/POPS membrane bilayers is not significant as indicated by ^{31}P and ^{2}H NMR (Lau et al. 2006). When incorporated, however, the upper part of the PC *sn*-1 palmitoyl chain becomes slightly more disordered. The formation of an isotropic spike in the ^{31}P spectra reflects the loss of membrane integrity and is similar to that observed for the fusogenic N-terminal region of the HIV-1 Nef protein (Curtain et al. 1994). The ^{31}P CSA also reduces significantly, suggesting more headgroup disorder and/or an average headgroup orientation, for example, which bends over more such that the choline moiety, under lipid long-axis rotation, swings closer to the interfacial strata. This may indicate a deeper membrane orientation for at least some of the Aβ(1–42) peptide which creates the extra space between lipid molecules and more room for the headgroup to swing.

We have also obtained peptide structure-related information in the context of lipid vesicles. The chemical shifts of selectively labelled Ala30 and Leu34 carbonyl ^{13}C of Aβ(1–42) showed an upfield shift upon association or incorporation with *d*POPC/POPS (Lau et al. 2007a, b). This is consistent with a conformational change from coiled to extended structures (Saitô 1983; Saitô et al. 1998), as shown also by CD for Aβ(1–42) in unilamellar vesicles of the same lipid composition (Lau et al. 2006) as well as Aβ(1–40) in dimyristoylphosphatidylcholine and dimyristoylphosphatidylglycerol unilamellar vesicles (Bokvist et al. 2004). However, as it was not clear whether the two carbonyl resonances corresponded to two different conformations or each carbonyl of the labelled pair, we have permuted the labelling pattern to include the α-^{13}C of Leu34 and the carbonyl ^{13}C of both Gly29 and Ala30. These two carbonyls are statistically likely to have the largest chemical shift difference of any two-carbonyl carbons (Biological Magnetic Resonance Data Bank 2007). Figure 6f–g shows a 4.1 ppm separation between the Gly29 and Ala30 carbonyl ^{13}C peaks, compared to <2 ppm observed under Ala30 and Leu34 carbonyl ^{13}C labelling. Thus the two resonances observed in both the current and previous reports (Lau et al. 2007a, b) are likely to represent two carbonyls that exist in a more uniform environment across the sample, rather than each resonance being characteristic of a different structural state.

Aβ(25–35) is a hydrophobic fragment from the C-terminal half of the full-length peptide and is neurotoxic to cortical cell cultures, yet lacks a metal-binding site. This toxicity suggests that the full-length peptide may have more than one mechanism of toxicity. Like the full-length peptide, Aβ(25–35) was found to influence lipid bilayers

differently depending on the method of addition. Peptide associated after *d*POPC/POPS vesicle formation was observed by ^{2}H NMR to only slightly reduce segmental order at both the top and bottom of the PC *sn*-1 palmitoyl chain. However, the peptide significantly increased the ^{31}P CSA while accelerating ^{31}P T_2 relaxation fivefold (Lau et al. 2007b), indicating an increase in order on the $\sim$100 μs and slow-motion limit time scales, and/or a more average orientation of the head group toward the membrane normal. Incorporation of Aβ(25–35) had a similar but less effect on lipid head group CSA while slowing T_2 relaxation slightly, and had an identical effect on the bottom of the acyl chain, but increased rather than decreased order at the top of the acyl chain. One interpretation is that Aβ(25–35) peptide is able to penetrate deeper into the interfacial region when incorporated during vesicle formation rather than associating afterward.

Using peptide analogously labelled to Aβ(1–42), $^{13}C\{^{1}H\}$ CPMAS data indicates that Aβ(25–35) similarly adopts a more extended conformation, regardless of the method of addition (Lau et al. 2007b). ^{13}C spectra in Fig. 6a–e, for a permutation of the labels for this peptide analogous to Aβ(1–42) as above, reinforce these conclusions; chemical shifts are consistent with a transition from coiled to extended peptide structure at positions 29 and 30 in going from dry to lipid-associated states, and this structure is invariant to mode of addition or cholesterol content (at 0 or 33%) in the bilayer.

As both peptides exhibit cytotoxicity, the shift toward extended conformation at the labelled C-terminal positions may be a required structural change which allows the peptide to perturb model membranes at the head group and interfacial regions, and in vivo to cause the disruption to nerve cell function. The commonality of these results for associated Aβ(1–42) and Aβ(25–35) with phospholipid bilayers suggests that a sequence tract which overlaps significantly with Aβ(25–35) may mediate an alternate toxic mechanism, which does not involve metals.

The effect of cholesterol and the drug Clioquinol (CQ)

Cholesterol is a rigid planar molecule, which orders membrane bilayers by inserting between the phospholipid molecules. The consequent increase in order corresponds to a decrease in the fluidity of the bilayers in both model and naturally derived bilayers (Brown and Seelig 1978; Stockton and Smith 1976; Suckling and Boyd 1976). As this ordering or stiffening of lipid bilayers could affect insertion of the peptide into the membrane (Chochina et al. 2001), we also included cholesterol in model membrane systems in our studies of Aβ peptide membrane interactions.

Cholesterol orders the *sn*-1 POPC chain by a factor of 1.9 and 1.6 at the upper CD_2 and terminal CD_3, respectively, in *d*POPC/POPS MLV bilayers as determined from the increase in the ^{2}H quadrupolar splitting for these acyl positions (Lau et al. 2007a, b). The ^{31}P CSA was reduced from −43 to −40 ppm with cholesterol, and T_2 relaxation rate was reduced from 6.2 to 10.6 ms. These perturbations are consistent with cholesterol occupying a position at the interfacial region of the membrane bilayer (Yeagle et al. 1975). Cholesterol consequently serves as a 'spacer' which allows head groups to lean over further on average (Yeagle et al. 1977) at the same time that the segmental motion of acyl chains are more restricted. The ordering effect appears also to translate to increased stability, as cholesterol protects the vesicle structure against Cu^{2+} destabilisation (Lau et al. 2007b).

The inclusion of Aβ peptide with *d*POPC/POPS/cholesterol MLV bilayers served in most cases to amplify the effect of cholesterol. Aβ(1–42) caused a further increase in acyl chain order, and decrease in headgroup ^{31}P CSA compared to cholesterol alone although ^{31}P T_2 relaxation times decreased from 10.6 to 4–5 ms (Lau et al. 2007a). Aβ(25–35) increased the acyl chain order slightly more than the full length peptide, but had little further apparent effect on the ^{31}P headgroup CSA (Lau et al. 2007a). Our new data, Fig. 6 demonstrates that both Aβ(1–42) and Aβ(25–35) peptides maintain similar conformations irrespective of the presence of cholesterol. Thus cholesterol appears in both cases to enable a deeper positioning of peptide within the membrane bilayers, without significant further perturbation of peptide structure, than when it is absent.

The effect of copper and Aβ(1–42) on lipid bilayers

Cu^{2+}, but not Zn^{2+}, was found to dramatically destabilise lipid vesicle bilayers at a mole ratio of 1:30 metal/lipid by both ^{31}P and ^{2}H SS-NMR (Lau et al. 2006). The addition of Cu^{2+} causes an apparent collapse of the static lineshape to an isotropic phase lipid, which clearly remains in the supernatant upon centrifugation and partitions from apparently intact vesicles. Aβ(1–42) clearly tightly binds the Cu^{2+} and effectually protects the membranes against the dramatic destabilisation at a peptide/metal ratio of 1:1. Remarkably, with respect to the effect of Aβ(1–42) alone on *d*POPC/POPS bilayers, the presence of Cu^{2+}, and to a lesser extent Zn^{2+}, Aβ(1–42) causes a large reduction in ^{31}P CSA. The overall effect is much greater when the Aβ(1–42) is incorporated during the vesicle formation than when associated afterward. Consistent with the inability of Aβ(25–35) to bind metals, the presence of Aβ(25–35) did not affect the impact of either Zn^{2+} or Cu^{2+} on membrane vesicles (Lau et al. 2007b).

Figure 7 demonstrates the profound influence Cu^{2+} ion has on the ^{13}C spectra of labelled Aβ(1–42) and Fig. 8 shows the effect on the ^{31}P spectra of the phospholipid headgroups. Upon addition of Cu^{2+}, a significant component from the intensity of Gly29 and Ala30 carbonyl ^{13}C chemical shifts move upfield from 170.4 and 174.5 ppm. Using calculated relative sideband intensities (Herzfeld 1980; Schmidt-Rohr 1994) for a ^{13}C carbonyl nucleus with $\delta = \sigma_z$ of 78 ppm and $\eta = (\sigma_y - \sigma_x)/\sigma_z \approx 0.92$ (Hartzell et al. 1987; Oas et al. 1987; Separovic et al. 1990; Stark et al. 1983), the spectra across MAS rates from 4 to 7 kHz are dominated by sideband manifolds arising from the Torlon (polyamide imide) MAS spacer, with three major components with centreband shifts of 122, 132, 166 ppm, and a fourth minor component at 138 ppm. The Cu^{2+}-broadened relaxation of the carbonyls from the C-terminal half of the peptide experience shifts under the anisotropic unpaired electron field (Aime et al. 1996; Kurland and McGarvey 1970), implying relatively structured proximity to the Cu^{2+}, although not necessarily by virtue of intramolecular folding. The Cα carbon of Leu34 at 52 ppm; however, was not significantly shifted or broadened, placing it possibly further from the complexed Cu^{2+}, particularly if this portion of the peptide maintains an extended structure as observed in the absence of Cu^{2+}.

Static ^{31}P NMR spectra of the same sample (Fig. 8) showed clear evidence of broadening, most likely owing to Cu^{2+}-induced T_2 relaxation, and the isotropic peak indicates formation of small vesicles, as previously reported for ^{31}P spectra of MLV devoid of cholesterol acquired without intervening MAS (Lau et al. 2006). In the present case, however, the isotropic peak was a consequence of relatively fast MAS as static ^{31}P spectra of Aβ(1–42) in *d*POPC/POPS/cholesterol with Cu^{2+} did not produce an isotropic peak (Lau et al. 2007a). This has also been observed in the case of the αM1 peptide in phospholipid bilayers (de Planque et al. 2004). As Cu^{2+} was added at stoichiometric levels to the peptide, which has a very tight binding constant for Cu^{2+} (Atwood et al. 2000), it is unlikely that there were significant levels of free Cu^{2+} available to associate with the phospholipid headgroups. Thus the ^{31}P broadening indicated that the peptide–Cu^{2+} complex is associated with the phospholipid headgroups, which may have possible disease implications for neuronal membranes. The evidence, therefore, suggests that a significant fraction of Gly29 and Ala30, but not Leu34, may be relatively close to the metal-binding sites in the lipid-associated form of peptide–Cu^{2+}. If so, this suggests that the membrane related structure of the peptide complexed with Cu^{2+} is different to the apo-peptide Aβ(1–40) fibril structure (Petkova et al. 2002), irrespective of whether the proximity to the metal is inter- or intramolecular in origin. Alternatively, the apparent influence of an unpaired electron may be caused by a specific radical species generated within the peptide (Kanski et al. 2001) or membrane.

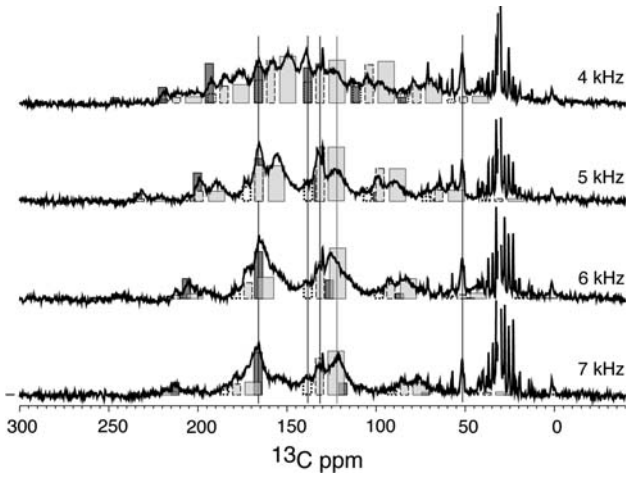

Fig. 7 ^{13}C CPMAS NMR spectra of Aβ(1–42)/POPC/POPS/cholesterol/$CuGly_2$ (1:10:10:10:1), at 150.8 MHz and four different MAS rates as indicated. Boxes indicate spectral components with spacing equivalent to the spinning speed, and relative heights proportional to theoretical sideband pattern for $\delta = 78$ ppm and $\eta = 0.92$ as described in the text. Components assigned to the Torlon MAS spacer are represented by: *wide light grey boxes* (centred at 122 ppm), *dashed light grey boxes* (centred at 132 ppm), *solid dark boxes* (centred at 166 ppm), and *dotted white boxes* (centred at 138 ppm). Leu34 is indicated at 52 ppm

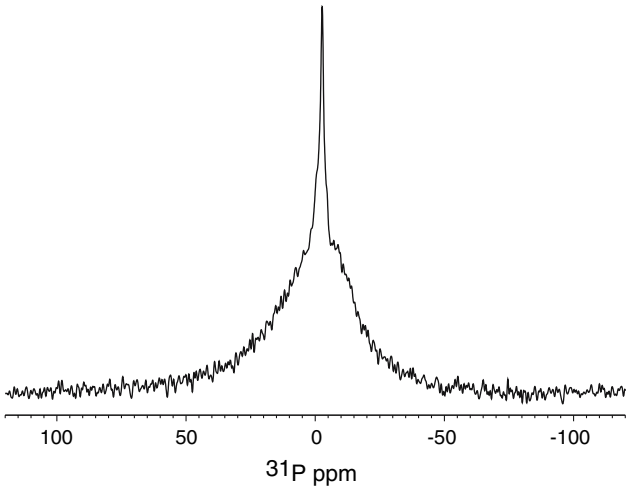

Fig. 8 Static ^{31}P NMR spectra of Aβ(1–42)/POPC/POPS/cholesterol/$CuGly_2$ (1:10:10:10:1) after spinning at 7 kHz at 14.1 T for $\sim$24 h. Narrow isotropic feature at $\sim$ −2 ppm has a shoulder, suggesting that this phase contains both POPC and POPS, and the broad, asymmetric feature appears to be both relaxation broadened (due to Cu^{2+}) and possibly representative of a distribution of different sized vesicles

The effect of CQ

The effect of the drug CQ on Aβ was also studied, as it has been demonstrated to have therapeutic potential (Barnham et al. 2003; Cherny et al. 2001, Tickler et al. 2005), based most obviously on its metal chelating properties. Significantly, however, CQ alone in *d*POPC/POPS MLV vesicle bilayers increased the phospholipid ^{31}P CSA from −43 to −49 ppm, corresponding to more order and/or a more upright headgroup orientation, and a likely positioning of CQ amongst the headgroups in the bilayer. The further addition of associated Aβ(1–42) appeared to have little effect on the CQ/bilayer interaction. When Cu^{2+} is included, however, the previously discussed narrowing of ^{31}P CSA by Aβ(1–42) in the presence of Cu^{2+} (−32 ppm) was increased (to −45 ppm), as if metal had been removed from the system with respect to peptide/metal/membrane interactions, but with a residual effect of CQ on the headgroups. Consequently, it is possible that CQ not only chelates metals rendering them unavailable to binding by Aβ(1–42), but the position of CQ within the membrane may also restrict membrane access of the peptide.

Conclusion

The Aβ(1–42) peptide, in the absence of metal, appeared to adopt an extended, β-strand type conformation and occupy a position in the lipid membrane amongst the lipid headgroups, probably reaching into the bilayer only as far as the interfacial region particularly in the presence of cholesterol. Cu^{2+}, which introduces an unpaired electon either directly or via oxidative mechanisms, clearly affected peptide carbonyl labels at Gly29 and/or Ala30 as well as ^{31}P nuclei in lipid headgroups, but not the Leu34 α-carbon nor lipid acyl chain ^{13}C nuclei. While the observed Aβ peptide is almost certainly not fibrilized nor otherwise aggregated into insoluble plaques, the oligomeric order of the "soluble" membrane-interacting peptide has yet to be determined. Further structural analysis of Aβ(1–42), including examination of metal effects in greater detail, is a topic of continuing work.

Acknowledgments The Australian Research Council is gratefully acknowledged for financial support by award of an ARC Discovery grant to FS and JDW. We thank John Hanna for helpful discussion.

References

Aime S, Bertini I, Luchinat C (1996) Considerations on high resolution solid state NMR in paramagnetic molecules. Coord Chem Rev 150:221–242

Ali FE, Barnham KJ, Barrow CJ, Separovic F (2004) Metal catalyzed oxidative damage and oligomerization of the amyloid-β peptide (Aβ) of Alzheimer's disease. Aust J Chem 57:511–518

Alzheimer A (1907) Über eigenartige Erkrankung der Hirinde. Allg Zschr Psychiat U Psychich-gerchtl Med 64:146–148

Andrew ER, Bradbury A, Eades RG (1958) Nuclear magnetic resonance spectra from a crystal rotated at high speed. Nature 182:1659

Andrew ER, Bradbury A, Eades RG (1959) Removal of dipolar broadening of nuclear magnetic resonance spectra of solids by specimen rotation. Nature 183:1802–1803

Arispe N, Doh M (2002) Plasma membrane cholesterol controls the cytotoxicity of Alzheimer's disease AbetaP (1–40) and (1–42) peptides. FASEB J 16:1526–1536

Atwood CS, Scarpa RC, Huang X, Moir RD, Jones WD, Fairlie DP, Tanzi RE, Bush AI (2000) Characterization of copper interactions with Alzheimer Aβ peptides: Identification of a attomolar affinity copper binding site on Aβ1–42. J Neurochem 75:1219–1233

Balla MS, Bowie JH, Separovic F (2004) Solid-state NMR study of antimicrobial peptides from Australian frogs in phospholipid membranes. Eur Biophys J 33:109–116

Brown MF, Seelig J (1978) Influence of cholesterol on the polar region of phosphatidylcholine and phosphatidylethanolamine bilayers. Biochemistry 17:381–384

Barnham KJ, Ciccotosto GD, Tickler AK, Ali FE, Smith DG, Williamson NA, Lam YH, Carrington D, Tew D, Kocak G, Volitakis I, Separovic F, Barrow CJ, Wade JD, Masters CL, Cherny RA, Curtain CC, Bush AI, Cappai R (2003) Neurotoxic, redox-competent Alzheimer's beta-amyloid is released from lipid membrane by methionine oxidation. J Biol Chem 178:42959–42965

Barnham KJ, Haeffner F, Ciccotosto GD, Curtain CC, Tew D, Mavros C, Beyreuther K, Carrington D, Masters CL, Cherny RA, Cappai R, Bush AI (2004) Tyrosine gated electron transfer is key to the toxic mechanism of Alzheimer's disease β-amyloid. FASEB J 18:1427–1429

Biological Magnetic Resonance Data Bank (2007) The University of Wisconsin, Madison. http://www.bmrb.wisc.edu. Cited 18 Aug 2007

Bokvist M, Lindström F, Watts A, Gröbner G (2004) Two types of Alzheimer's β-amyloid (1–40) peptide membrane interactions: aggregation preventing transmembrane anchoring versus accelerated surface fibril formation. J Mol Biol 335:1039–1049

Burdick D, Soreghan B, Kwon M, Kosmoski J, Knauer M, Henschen A, Yates J, Cotman C, Glabe C (1992) Assembly and aggregation properties of synthetic Alzheimer's A4/beta amyloid peptide analogs. J Biol Chem 267:546–554

Bush AI (2003) The metallobiology of Alzheimer's disease. Trends Neurosci 26:207–214

Cherny RA, Atwood CS, Xilinas ME, Gray DN, Jones WD, McLean CA, Barnham KJ, Volitakis I, Fraser FW, Kim Y, Huang X, Goldstein LE, Moir RD, Lim JT, Beyreuther K, Zheng H, Tanzi RE, Masters CL, Bush AI (2001) Treatment with a copper-zinc chelator markedly and rapidly inhibits beta-amyloid accumulation in Alzheimer's disease transgenic mice. Neuron 30:665–676

Chochina SV, Avdulov NA, Igbavboa U, Cleary JP, O'Hare EO, Wood WG (2001) Amyloid beta-peptide 1–40 increases neuronal membrane fluidity: role of cholesterol and brain region. J Lipid Res 42:1292–1297

Choo-Smith LP, Garzon-Rodriguez W, Glabe CG, Surewicz WK (1997) Acceleration of amyloid fibril formation by specific binding of A beta-(1–40) peptide to ganglioside-containing membrane vesicles. J Biol Chem 272:22987–22990

Christian H, Simon G, Victor AG, Patrick H, Mallot HA (2007) Soluble beta-amyloid[25–35] reversibly impairs hippocampal

synaptic plasticity and spatial learning. Eur J Pharmacol 561:85–90
Coles M, Bicknell W, Watson AA, Fairlie DP, Craik DJ (1998) Solution structure of amyloid beta-peptide(1–40) in a water-micelle environment. Is the membrane-spanning domain where we think it is? Biochemistry 37:11064–11077
Cornell BA, Hiller RG, Raison J, Separovic F, Smith R, Vary JC, Morris C (1983) Biological membranes are rich in low frequency motion. Biochim Biophys Acta 732:473–478
Cornell BA, Weir LE, Separovic F (1988) The effect of gramicidin A on phospholipid bilayers. Eur Biophys J 16:113–119
Curtain CC, Separovic F, Rivett D, Kirkpatrick A, Waring AJ, Gordon LM, Azad AA (1994) The amino-terminal region of the HIV-1 Nef protein is fusogenic. AIDS Res Hum Retroviruses 10:1231–1240
Demeester N, Baier G, Enzinger C, Goethals M, Vandekerckhove J, Rosseneu M, Labeur C (2000) Apoptosis induced in neuronal cells by C-terminal amyloid β-fragments is correlated with their aggregation properties in phospholipid membranes. Mol Membr Biol 17:219–228
de Planque MRR, Rijkers DTS, Fletcher J, Liskamp RMJ, Separovic F (2004) The αM1 segment of the nicotinic acetylcholine receptor exhibits conformational flexibility in a membrane environment. Biochim Biophys Acta 1665:40–47
Donnelly PS, Xiao Z, Wedd AG (2007) Copper and Alzheimer's disease. Curr Opin Chem Biol 11:128–133
Dufourc EJ, Mayer C, Stohrer J, Althoff G, Kothe G (1992) Dynamics of phosphate head groups in biomembranes. Comprehensive analysis using phosphorus-31 nuclear magnetic resonance lineshape and relaxation time measurements. Biophys J 61:42–57
Fassbender K, Masters C, Beyreuther K (2001) Alzheimer's disease: molecular concepts and therapeutic targets. Naturwissenschaften 88:261–267
Fung BM, Khitrin AK, Ermolaev K (2000) An improved broadband decoupling sequence for liquid crystals and solids. J Magn Reson 142:97–101
Gehman JD, Separovic F (2006) Solid-State NMR of Membrane-Active Proteins and Peptides. In: Webb GA (ed) Modern magnetic resonance. Springer, Heidelberg, pp 301–307
Gehman JD, Separovic F, Lu K, Mehta AK (2007) Boltzmann statistics rotational-echo double-resonance analysis. J Phys Chem B 111:7802–7811
Glenner GG, Wong CW (1984) Alzheimer's disease: Initial report of the purification and characterization of a novel cerebrovascular amyloid protein. Biochem Biophys Res Commun 120:885–890
Griffin RG, Powers L, Pershan PS (1978) Head-group conformation in phospholipids: a phosphorus-31 nuclear magnetic resonance study of oriented monodomain dipalmitoylphosphatidylcholine bilayers. Biochemistry 17:2718–2722
Harper JD, Lansbury PT Jr (1997) Models of amyloid seeding in Alzheimer's disease and scrapie: mechanistic truths and physiological consequences of the time-dependent solubility of amyloid proteins. Annu Rev Biochem 66:385–407
Hartley DM, Walsh DM, Ye CP, Diehl T, Vasquez S, Vassilev PM, Teplow DB, Selkoe DJ (1999) Protofibrillar intermediates of amyloid beta-protein induce acute electrophysiological changes and progressive neurotoxicity in cortical neurons. J Neurosci 19:8876–8884
Hartzell CJ, Whitfield M, Oas TG, Drobny GP (1987) Determination of the 15N and 13C chemical shift tensors of L-[13C]alanyl-L-[15N]alanine from the dipole-coupled powder patterns. J Am Chem Soc 109:5966–5969
Herzfeld J, Griffin RG, Haberkorn RA (1978) Phosphorus-31 chemical-shift tensors in barium diethyl phosphate and urea-phosphoric acid: model compounds for phospholipid head-group studies. Biochemistry 17:2711–2718
Herzfeld J, Berger AE (1980) Sideband intensities in NMR spectra of samples spinning at the magic angle. J Chem Phys 73:6021–6030
Jick J, Zornberg GL, Jick SS, Seshadri S, Drachman DA (2000) Statins and the risk of dementia. Lancet 356:1627–1631
Kang J, Lemaire HG, Unterbeck A, Salbaum JM, Masters CL, Grzeschik KH, Multhaup G, Beyreuther K, Muller-Hill B (1987) The precursor of Alzheimer's disease amyloid A4 protein resembles a cell-surface receptor. Nature 325:733–736
Kanski J, Varadarajan S, Aksenova M, Butterfield DA (2001) Role of glycine-33 and methionine-35 in Alzheimer's amyloid β-peptide 1–42-associated oxidative stress and neurotoxicity. Biochim Biophys Acta 1586:190–198
Kayed R, Head E, Thompson JL, McIntire TM, Milton SC, Cotman CW, Glabe CG (2003) Common structure of soluble amyloid oligomers implies common mechanism of pathogenesis. Science 300:486–489
Kohler SJ, Klein MP (1976) 31P nuclear magnetic resonance chemical shielding tensors of phosphorylethanolamine, lecithin, and related compounds: applications to head-group motion in model membranes. Biochemistry 15:967–974
Kohler SJ, Klein MP (1977) Orientation and dynamics of phospholipid head groups in bilayers and membranes determined from 31P nuclear magnetic resonance chemical shielding tensors. Biochemistry 16:519–526
Kurland RJ, McGarvey BR (1970) Isotropic NMR shifts in transition metal complexes: the calculation of the Fermi contact and pseudocontact terms. J Magn Reson 2:286–301
Lambert MP, Barlow AK, Chromy BA, Edwards C, Freed R, Liosatos M, Morgan TE, Rozovsky I, Trommer B, Viola KL, Wals P, Zhang C, Finch CE, Krafft GA, Klein WL (1998) Diffusible, nonfibrillar ligands derived from Aβ1–42 are potent central nervous system neurotoxins. Proc Natl Acad Sci USA 95:6448–6453
Lau T-L, Barnham KJ, Curtain CC, Masters CL, Separovic F (2003) Magnetic resonance studies of the β-amyloid peptide. Aust J Chem 56:349–356
Lau T-L, Ambroggio EE, Tew DJ, Cappai R, Masters CL, Fidelio GD, Barnham KJ, Separovic F (2006) Amyloid-β peptide disruption of lipid membranes and the effect of metal ions. J Mol Biol 356:759–770
Lau T-L, Gehman JD, Wade JD, Masters CL, Barnham KJ, Separovic F (2007a) Cholesterol and Clioquinol modulation of Aβ(1–42) interaction with phospholipids bilayers and metals. Biochim Biophys Acta 1768:2400–2408
Lau T-L, Gehman JD, Wade JD, Perez K, Masters CL, Barnham KJ, Separovic F (2007b) Membrane interactions and the effect of metal ions of the amyloidogenic fragment Aβ(25–35) in comparison to Aβ(1–42). Biochim Biophys Acta 1768:2400–2408
Lesné S, Koh MT, Kotilinek L, Kayed R, Glabe CG, Yang A, Gallagher M, Ashe KH (2006) A specific amyloid-β protein assembly in the brain impairs memory. Nature 440:352–357
Lowe IJ (1959) Free induction decays of rotating solids. Phys Rev Lett 2:285–287
Maricq MM, Waugh JS (1979) NMR in rotating solids. J Chem Phys 70:3300–3316
Masters CL, Simms G, Weinman NA, Multhaup G, McDonald BL, Beyreuther K (1985) Amyloid plaque core protein in Alzheimer disease and down syndrome. Proc Natl Acad Sci 82:4245–4249
McLean CA, Cherny RA, Fraser FW, Fuller SJ, Smith MJ, Beyreuther K, Bush AI, Masters CL (1999) Soluble pool of Aβ amyloid as a determinant of severity of neurodegeneration in Alzheimer's disease. Ann Neurol 46:860–866
Mehring M (1983) Principles of high resolution NMR in solids. Springer, Heidelberg

Oas TG, Hartzell CJ, McMahon TJ, Drobny GP, Dahlquist FW (1987) The carbonyl 13C chemical shift tensors of five peptides determined from 15N dipole-coupled chemical shift powder patterns. J Am Chem Soc 109:5956–5962

Pake GE (1948) Nuclear resonance absorption in hydrated crystals: fine structure of the proton line. J Chem Phys 16:327–336

Petkova AT, Ishii Y, Balbach JJ, Antzutkin ON, Leapman RD, Delaglio F, Tycko R (2002) A structural model for Alzheimer's beta-amyloid fibrils based on experimental constraints from solid state NMR. Proc Natl Acad Sci USA 99:16742–16747

Roher AE, Lowenson JD, Clarke S, Woods AS, Cotter RJ, Gowing E, Ball MJ (1993) β-Amyloid-(1–42) is a major component of cerebrovascular amyloid deposits: implications for the pathology of Alzheimer disease. Proc Natl Acad Sci USA 90:10836–10840

Saitô H (1983) Conformation-dependent 13C chemical shifts: a new means of conformational characterization as obtained by high-resolution solid-state NMR. Magn Reson Chem 24:835–852

Saitô H, Tuzi S, Yamaguchi S, Kimura S, Tanio M, Kamihira M, Nishimura K, Naito A (1998) Conformation and dynamics of membrane proteins and biologically active peptides as studied by high-resolution 13C NMR. J Mol Struct 441:137–148

Schmidt-Rohr K, Spiess HW (1994) Multidimensional solid-state NMR and polymers. Academic Press, San Diego

Seelig J, Gally H (1976) Investigation of phosphatidylethanolamine bilayers by deuterium and phosphorus-31 nuclear magnetic resonance. Biochemistry 15:5199–5204

Separovic F, Smith R, Yannoni CS, Cornell BA (1990) Molecular sequence effect on the 13C carbonyl chemical shift shielding tensor. J Am Chem Soc 112:8324–8328

Separovic F, Cornell B, Pace R (2000) Orientation dependence of NMR relaxation time, $T_{1\rho}$, in lipid bilayers. Chem Phys Lipids 107:159–167

Separovic F, Drechsler A, Lau T-L (2004) Magnetic moments: membrane protein structures by NMR. Chem Aust 71(1):4–7

Singer SJ, Nicolson GL (1972) The fluid mosaic model of the structure of cell membranes. Science 175:720–731

Sisodia SS (1992) β-Amyloid precursor protein cleavage by a membrane-bound protease. Proc Natl Acad Sci USA 89:6075–6079

Smith DP, Smith DG, Curtain CC, Boas JF, Pilbrow JR, Ciccotosto GD, Lau T-L, Tew DJ, Perez K, Wade JD, Bush AI, Drew SC, Separovic F, Masters CL, Cappai R, Barnham KJ (2006) Copper-mediated amyloid-β toxicity is associated with an intermolecular histidine bridge. J Biol Chem 281:15145–15154

Smith DG, Cappai R, Barnham KJ (2007) The redox chemistry of the Alzheimer's disease amyloid beta peptide. Biochim Biophys Acta 1768:1976–1990

Sparks DL, Hunsaker JC, Scheff SW, Kryscio RJ, Henson JL, Markesbery WR (1990) Cortical senile plaques in coronary artery disease, aging and Alzheimer's disease. Neurobiol Aging 11:601–607

Stark RE, Jelinski LW, Ruben DJ, Torchia DA, Griffin RG (1983) 13C chemical shift and 13C-15N dipolar tensors for the peptide bond: [1–13C]glycyl[15N]glycine·HCl·H_2O. J Magn Reson 55:266–273

Stejskal EO, Schaefer J, Waugh JS (1977) Magic-angle spinning and polarization transfer in proton-enhanced NMR. J Magn Reson 28:105–112

Stockton GW, Smith IC (1976) A deuterium nuclear magnetic resonance study of the condensing effect of cholesterol on egg phosphatidylcholine bilayer membranes. I. Perdeuterated fatty acid probes. Chem Phys Lipids 17:251–263

Subasinghe S, Unabia S, Barrow CJ, Mok SS, Aguilar MI, Small DH (2003) Cholesterol is necessary both for the toxic effect of Abeta peptides on vascular smooth muscle cells and for Abeta binding to vascular smooth muscle cell membranes. J Neurochem 84:471–479

Suckling KE, Boyd GS (1976) Interactions of the cholesterol side-chain with egg lecithin. A spin label study. Biochim Biophys Acta 436:295–300

Tickler AK, Wade JD, Separovic F (2005) The role of A beta peptides in Alzheimer's disease. Protein Peptide Lett 12:513–519

Varadarajan S, Kanski J, Aksenova M, Lauderback C, Butterfield DA (2001) Different mechanisms of oxidative stress and neurotoxicity for Alzheimer's A beta(1–42) and A beta(25–35). J Am Chem Soc 123:5625–5631

Watwe RM, Bellare JR (1995) Manufacture of liposomes—a review. Curr Sci 68:715–724

Yeagle PL, Hutton WC, Huang CH, Martin RB (1975) Headgroup conformation and lipid- cholesterol association in phosphatidylcholine vesicles: a 31P{1H} nuclear Overhauser effect study. Proc. Natl Acad Sci USA 72:3477–3481

Yeagle PL, Hutton WC, Huang CH, Martin RB (1977) Phospholipid head-group conformations; intermolecular interactions and cholesterol effects. Biochemistry 16:4344–4349

Zhang Y, McLaughlin R, Goodyer C, LeBlanc A (2002) Selective cytotoxicity of intracellular amyloid β peptide$_{1-42}$ through p53 and Bax in cultured primary human neurons. J Cell Biol 156:519–529